arXiv:1701.04726v1 [cond-mat.dis-nn] 17 Jan 2017

Directed negative-weight percolation

C. Norrenbrock,* M. M. Mkrtchian,† and A. K. Hartmann‡
Institut für Physik, Universität Oldenburg, 26111 Oldenburg, Germany
(Dated: January 18, 2017)

We consider a directed variant of the negative-weight percolation model in a two-dimensional, periodic, square lattice. The problem exhibits edge weights which are taken from a distribution that allows for both positive and negative values. Additionally, in this model variant all edges are directed. For a given realization of the disorder, a minimally weighted loop/path configuration is determined by performing a non-trivial transformation of the original lattice into a minimum weight perfect matching problem. For this problem, fast polynomial-time algorithms are available, thus we could study large systems with high accuracy. Depending on the fraction of negatively and positively weighted edges in the lattice, a continuous phase transition can be identified, whose characterizing critical exponents we have estimated by a finite-size scaling analyses of the numerically obtained data. We observe a strong change of the universality class with respect to standard directed percolation, as well as with respect to undirected negative-weight percolation. Furthermore, the relation to directed polymers in random media is illustrated.

PACS numbers: 64.60.Ak,75.40.Cx,68.35.Rh
Keywords:

I. INTRODUCTION

In statistical physics, one of the central targets is to study systems that exhibit continuous phase transitions. Due to the diverging correlation length in the critical region, long-range correlations are not affected by details of microscopic interactions, but depend on symmetry properties of the underlying model only. For that reason models that exhibit continuous phase transition can be grouped in universality classes, which are characterized by a set of critical exponents and their functional relations, i.e. scaling laws [1]. One of the most basic and intensively studied universality classes is that of standard percolation [2, 3], which addresses the question of connectivity. Based on a tunable parameter p, sites or links in a given lattice get occupied or stay empty. Then, the central objects of interest are clusters consisting of adjacent and occupied sites. Above a certain value of $p = p_c$, i.e. the critical point, a lattice-spanning cluster emerges in the thermodynamic limit. Even the model is probably the simplest possible model exhibiting a phase transition, its importance comes from the following facts. First, it allows to study basically all fundamental aspects of phase transitions within a very basic framework. Second, many much more complex phase transitions can be traced back to an underlying percolation transition, e.g., the percolation of Fortuin-Kasteleyn clusters [4] in the Ising model.

In standard percolation, there is no directional information in the connectivity pattern. Thus, not surprisingly, the critical exponents describing this phase transition differ from those that describe the phase transition in directed percolation (DP) [5], which is a variant of standard percolation, where the links carry a direction, leading to an anisotropic behavior. Note that this directionality can be interpreted as time direction, making DP relevant for the description of non-equilibrium processes. In particular, because of the anisotropic nature of the cluster building process in DP, correlations are not governed by one but two correlation lengths: $\xi_\parallel$ and $\xi_\perp$.

Also, in standard percolation, the links do not carry any weights, thus, one can assume all weights being one, i.e., they are in particular positive. Recently, a percolation model called "negative-weight percolation" (NWP) was introduced [6], where random weights are attached to the links, and, in particular, weights of either sign are allowed. Algorithmically, this means special global optimization polynomial-time "matching" algorithms have to applied, see Sec. II. This leads, interestingly, to a new type of behavior giving rise to a different universality class compared to standard percolation. In a series of papers [7–13], NWP has been studied in different dimensions and different variants.

It has been shown that two distinct phases can be identified depending on a disorder parameter ρ, which controls the amount of negative weights. (i) for small ρ the geometric objects are rather small and straight-lined, which reflects a self-affine scaling, (ii) for large ρ the geometric objects scale self-similar and can wind around the lattice. In Ref. [6] the disorder-driven phase transition was investigated by means of finite-size scaling analyses and it turned out that the critical exponents were universal in 2D (different lattice geometries and disorder distribution were studied). Further studies regarding isotropic NWP address the influence of dilution on the critical properties [7], the upper critical dimension ($d_u = 6$) [8], another upper critical dimension ($d_u^{\mathrm{DPL}} = 3$) for densely packed loops far above the critical point [9], the mean-field behavior on a random graph with fixed connectivity

*Electronic address: christoph.norrenbrock@uni-oldenburg.de
†Electronic address: mitchell.mger.mkrtchian@uni-oldenburg.de
‡Electronic address: alexander.hartmann@uni-oldenburg.de

[10], the Schramm-Loewner evolution properties of paths in 2D lattices [12], and loop-length distributions in several dimensions [11].

Nevertheless, all this work was for non-directed lattices or graphs. Thus, as compared to the change which occurs when moving from standard to directed percolation, it is valid to ask whether the directed variant of NWP, which is introduced and studied in this work, gives again rise to a new type of behavior.

Note that, while DP is defined as a local growth process, the path-like clusters in NWP emerge due to global optimization. This is also true for directed polymers in random media (DPRM) [14], but unlike NWP, DPRM does not feature a phase transition. Nevertheless, it will be outlined in this article that NWP and DPRM are partially related to each other.

Next, we outline the model and the numerical procedures. NWP can be defined on any graph, in particular finite-dimensional lattices, which we consider here. In particular we study here a directed, weighted, periodic, simple square lattices with side length L. The direction of the edges is arranged as follows: All horizontal edges point to the left and all vertical ones point up. Edge weights are drawn from a distribution which provides both positive and negative values. The proportion of negative and positive weights can be tuned by a disorder parameter ρ.

We study paths and loops in the lattice. For each path or loops a weight is defined which consist of the sum of the weights of the edges contributing to the loop or path. For a given realization of the disorder, an *optimal* configuration consisting of one path and zero or possibly a finite number of system-spanning loops is determined. The configuration must fulfill some constrains: The path must be fixed at the bottom right, the loops and the path are not allowed to intersect one another, and the total sum of all weights of the loops and the path must be an exact *minimum*. The algorithm is very similar to the undirected case, the changes which are necessary are explained in Sec. II.

Fig. 1 shows such optimal configurations for different values of ρ in a lattice of size $L = 32$. The main question we are interested in is, whether there is a system spanning path or system spanning loops, i.e., whether at least one object percolates. Note that for analyzing geometrical properties we are using the path. The loops arise (unavoidably) from the global nature of the underlying optimization problem, see the technical details in Sec. III and allow us to study the percolation transition at $\rho = \rho_c$, i.e., whether the full lattice admits one or several percolating objects. Note that here, due to the construction of the underlying lattice with directed edges, small loops can not occur, in contrast to the undirected NWP. In particular, this is true for $\rho < \rho_c$ (cf. Fig. 1(a)) where just a finite path appears and loops are absent. At the critical point $\rho = \rho_c$ there appears a lattice-spanning loop in the depicted example Fig. 1(b), since there are enough negatively weighted edges in the lattice. Also a percolating path and no percolating loop might appear for some realizations. Above the critical point $\rho > \rho_c$ the number of lattice-spanning loops increases and even the path winds around the lattice (cf. Fig. 1(c)). Thus, this article we study the disorder-driven, geometric phase transition and determine its characterizing critical exponents, in particular with respect to the parallel and perpendicular correlation lengths.

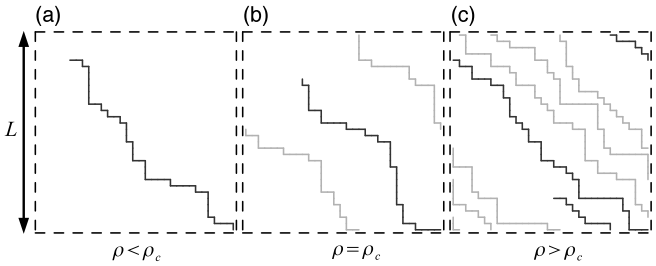

FIG. 1: Illustration of minimum-weight configurations consisting of loops (gray) and one path (black) in a directed 2D square lattice of side length $L = 32$ with periodic boundary conditions. The path is forced to start at the right bottom corner. For small values of ρ, there does not appear a loop and also the path does not span the lattice. At $\rho = \rho_c$ one percolating loop occurs. For large values of ρ, there are many spanning loops and also the path is percolating.

As an interpretation of the NWP problem, one can imagine an agent that takes a trip in a graph along the path.Whenever he travels along a positively weighted edge, the agent has to pay some resource according to the positive value. On the other hand, he will harvest some resource, if he travels along a negatively weighted edge. Therefore, the optimal path/loop configuration obtained in the context of the NWP problem provides the optimal route of the agent (path), possibly in competition with other agents (loops), to gain as many resources as possible. Only paths or loops which lead to a larger amount of harvested resources as compared to the paid resources will occur.

The remainder of this article is organized as follows. In Sec. II, we introduce the model in more detail and explain the algorithm. In Sec. III, we describe the finite-size scaling technique that has been used to estimate the critical exponents numerically and present our results. We close with a summary in Sec. IV.

II. MODEL AND ALGORITHM

The underlying graph $G = (V, E)$ at hand is a 2D directed square lattice whose edges point either to the left or up. Its boundaries are periodic meaning the lattice can be considered as placed on a torus in a topological sense. Each edge $e_{ij} \in E$ carries a weight ω_{ij} that is taken from a "Gauss-like" distribution characterized by

a tunable disorder parameter ρ:

$$P(\omega) = (1-\rho)\delta(\omega-1) + \rho\exp(-\omega^2)/\sqrt{2\pi}, \quad 0 \le \rho \le 1. \quad (1)$$

The shape of the lattice is quadratic in all simulations, so the number of nodes is $N = |V| = L^2$.

Given such a graph and a realization of the disorder, an optimal configuration consisting of an arbitrary number of loops, i.e., closed paths, and one additional path (possibly with zero length is computed. The configuration must fulfill following requirements: i) One endpoint of the path must be pinned at the bottom right corner. However, it is also allowed that no path occurs. ii) The loops and the paths are not allowed to cross or touch each other. iii) The configurational energy

$$\mathcal{E} = \sum_{\mathcal{L}\in\mathcal{C}} \omega_{\mathcal{L}} \quad (2)$$

has to be minimized. Here $\omega_{\mathcal{L}}$ denotes the total of all edge weights belonging to loop or path $\mathcal{L}$. Note that Eq. 1 provides real numbers, so the optimal configuration is unique for each realization of the disorder. Since the number of loops is not specified and even the path might not appear (zero length), also an empty configuration might be valid. This would be the case, e.g., if all edges carried a positive weight. Loops and also the path can solely appear, if their weight is negative, otherwise $\mathcal{E}$ would not be minimal, since an empty configuration has $\mathcal{E} = 0$. Furthermore, since all edges point either to the left or up, loops can appear only, if they span the lattice in either horizontal or vertical direction. Therefore, their smallest length is L. As a matter of fact, the typical length of the loops is $2L$ in the vicinity of the critical point.

In order to find the optimal configuration, we transform the original graph to an appropriate auxiliary graph first. Subsequently, a *minimum-weight perfect matching* (MWPM) [15–17] provides all information to reconstruct the original graph exhibiting the correct loop/path configuration. Fig. 2 is an illustration of the algorithmic procedure for a given realization of the disorder for a periodic lattice of size $L = 3$. For reasons of clarity, only loops but no path can occur here. Guided by Fig. 2, we give a concise description how the algorithm works. Afterwards, we explain in which way the algorithm must be altered, so that the appearance of a path becomes possible.

(1) First all original nodes are *duplicated*. For each pair of duplicated nodes, one additional edge with zero weight is added linking both nodes of a pair. The two duplicated nodes of one pair (represented black and white in Fig. 2(b)) are treated differently. Considering just one pair, if an adjacent edge has pointed to the original node, this edge will be linked to one of the duplicated nodes (in Fig. 2(b) this node is the black one). On the other hand, if the edge has pointed away from the original node, it will be connected to the other duplicated node (in Fig. 2, this node is white). Subsequently, each of the original edges is replaced by a path of three edges and two *additional* nodes (in Fig. 2(b), these nodes are depicted as squares). One of the two edges that are connected with the duplicates of the original nodes is assigned with the weight of the original edge. The other two edges carry zero weight. The resulting auxiliary graph is illustrated in Fig. 2(b), where bold edges carry the original weights and the thin ones carry a weight of zero. A more extensive and pedagogical description of the mapping (for the undirected variant of the model, where the auxiliary graph is slightly different) can be found in Ref. [18].

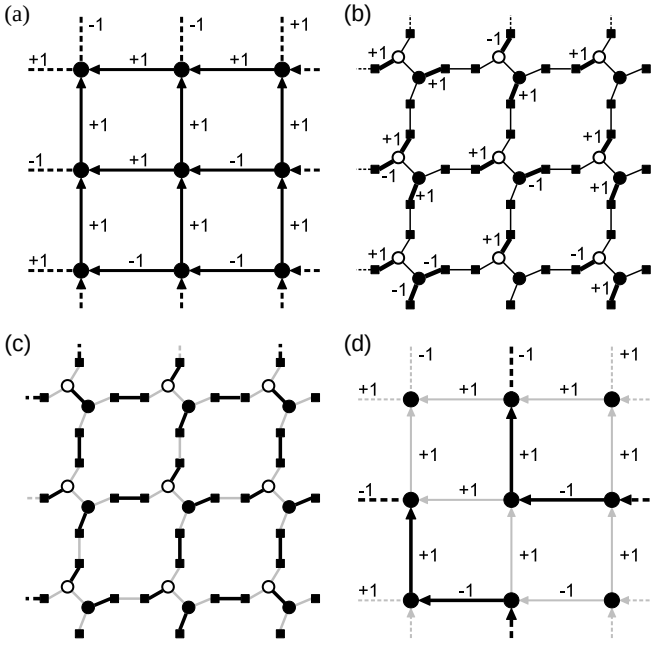

FIG. 2: Illustration of the algorithmic procedure for a periodic lattice of size $L = 3$. For the sake of clarity, the procedure is just depicted for a directed lattice that does not contain a finite path. In Sec. II it is described how the construction of the auxiliary graph must be altered in order to force a path in the lattice that starts at the bottom right corner and terminates at any node. (a) Original lattice with weighted, directed edges. (b) Auxiliary graph with proper weight assignment. The thick edges carry the weight as the respective edges in the original graph. The weights of all other edges are zero. (c) Illustration of the MWPM: black edges are matched and gray ones are unmatched. For the sake of clarity, edge weights are not depicted. (d) Reconstruction to the original lattice taking the MWPM result into account.

(2) A MWPM is determined on the auxiliary graph via exact combinatorial optimization algorithms [19]. A perfect matching is a subset of edges M which ensures that each node in the graph has exactly one incident edge $\in M$. There are several subsets that fulfill this condition. The MWPM is that perfect matching which has the lowest total weight. For the given example, the MWPM is illustrated in Fig. 2(c). Edges that belong to the MWPM are represented bold and black.

(3) After determining the MWPM, the original graph can be reconstructed. If and only if the edge that links two additional nodes (in Fig. 2(c) these nodes are illustrated as squares) does belong to the MWPM, the corresponding edge in the original graph is not part of the optimal loop/path configuration. If, on the other hand, the two additional nodes are not matched to each other, by the definition of the MWPM, they have to be matched to duplicated nodes, respectively. In this case the corresponding edge of the original graph is part of a loop. In this way the complete optimal loop/path configuration can be determined. In the presented example (cf. Fig. 2(d)) the optimal configuration consists of one loop with total weight -2.

As the algorithm has been presented, it is not possible to find a path that is pinned in the bottom right corner. In order to enable such a path, the auxiliary graph must be expanded. After constructing the auxiliary graph as described above, the white duplicate of the original node in the bottom right corner gets connected via a path consisting of three edges (all carry zero weight) and two nodes to the black duplicates of all other original nodes. This means technically the path is also a loop, but the "returning" part of the loop is "hidden" with respect to the original lattice, such that it appears as a path there. Such an auxiliary graph is not planar and contains many additional edges, therefore, we do not depict this additional specification in the illustration Fig. 2.

III. RESULTS

The NWP model exhibits a geometrical continuous phase transition. For a small amount of negative weights, the path would appear rather short and loops would not appear at all, if the system size were chosen sufficiently large. This can be seen in Fig. 1. For small values of ρ, the formation of loops is suppressed, because each possible loop has length $O(L)$ and thus would collect too many positively weighted edges. This is clearly different in the undirected variant of the model, where also small loops will appear, even if ρ is small [6]. On the other hand, if ρ is large, the path might grow very long and even multiple loops will occur.

The two regions, in which lattice-spanning, i.e., percolating, loops or paths will or, respectively, will not occur with high probability, are separated by a certain value of $\rho = \rho_c(L)$, the critical point. In the thermodynamic limit, i.e., $L \to \infty$, there are no lattice-spanning objects in the lattice, if $\rho < \rho_c = \rho_c(\infty)$. On the other hand, if $\rho > \rho_c$, there will appear some percolating objects always.

In this section we determine the critical point and estimate the critical exponents that characterize the phase transition via a finite-size scaling analysis. Note that a common scaling assumption [3] that is typically used for undirected models cannot be applied here. Therefore, due to the anisotropic nature of the underlying lattice (parallel and perpendicular to the natural diagonal orientation), there are two different correlation lengths that have a different asymptotic behavior

$$\xi_\parallel \sim |\rho - \rho_c|^{-\nu_\parallel}, \qquad \xi_\perp \sim |\rho - \rho_c|^{-\nu_\perp} \tag{3}$$

in the thermodynamic limit, with $\nu_\parallel$ and $\nu_\perp$ being the critical exponents describing the power-law divergence of the correlation lengths, respectively. At the critical point, their finite-size scaling is assumed to be [20]

$$\begin{aligned} \xi_\parallel &\sim L^{\theta_\parallel} \\ \xi_\perp &\sim L^{\theta_\perp}. \end{aligned} \tag{4}$$

For anisotropic percolation models a phenomenological finite-size scaling theory is introduced in Ref. [20]. It is expected that cluster related quantities $y(L, \rho)$ can be rescaled according to

$$\begin{aligned} y(L,\rho) &= L^{-b\,\theta_\parallel/\nu_\parallel} f[(\rho - \rho_c) L^{\theta_\parallel/\nu_\parallel}] \\ &= L^{-b\,\theta_\perp/\nu_\perp} f[(\rho - \rho_c) L^{\theta_\perp/\nu_\perp}], \end{aligned} \tag{5}$$

where $f[\cdot]$ is an unknown scaling function and b represents a dimensionless critical exponent that describes the asymptotic behavior of $y(L, \rho)$ in the thermodynamic limit. According to Eq. 5, if ρ_c, $\theta_\parallel/\nu_\parallel$ and b are chosen properly, all data points of $y(L,\rho)L^{b\,\theta_\parallel/\nu_\parallel}$ have to lie on one single curve. Therefore, $y(L, \rho)$ can be measured numerically for different values of L and ρ and, subsequently, $y(L,\rho)L^{b\,\theta_\parallel/\nu_\parallel}$ can be plotted against $(\rho - \rho_c)L^{\theta_\parallel/\nu_\parallel}$. Then, the unknown constants ρ_c, $\theta_\parallel/\nu_\parallel$ and b can be adjusted until the data "collapses" to one curve indicating that the correct values of the constants are found. The same also applies for $\theta_\perp/\nu_\perp$ instead of $\theta_\parallel/\nu_\parallel$. Note, that Eq. 5 shows the scaling behavior of systems that are sufficiently large only [21]. All data collapses in this article are made with a computer-assisted scaling analysis [22].

This data collapse approach allows only to determine the ratios $\theta_\perp/\nu_\perp$ and $\theta_\parallel/\nu_\parallel$. In order to find an estimate for $\nu_\parallel$ and $\nu_\perp$, we additionally determine $\theta_\parallel$ and $\theta_\perp$ directly by applying Eqs. 4. For that reason, the path is forced on the lattice, because, as evident from Fig. 3(a), the correlation lengths can be estimated by taking measurements of the path. The measurements are taken at the estimated critical point $\rho_c = 0.3789$ that has been found with the data collapse technique described above and will be presented below. For the ease of presentation, we do not have to deal with the ratios θ/ν, we have switched the order here and show the determination of $\theta_\parallel$ and $\theta_\perp$ first. Fig. 3(b) shows that a very clean power law behavior is visible, leading to $\theta_\parallel = 0.83(2)$ and $\theta_\perp = 0.53(2)$.

To actually determine the critical point and obtain the other critical exponents, we have monitored several observables in the vicinity of the expected value of the critical point ($p \in [0.377, 0.382]$) for different system sizes. Since we could use fast optimization algorithms,

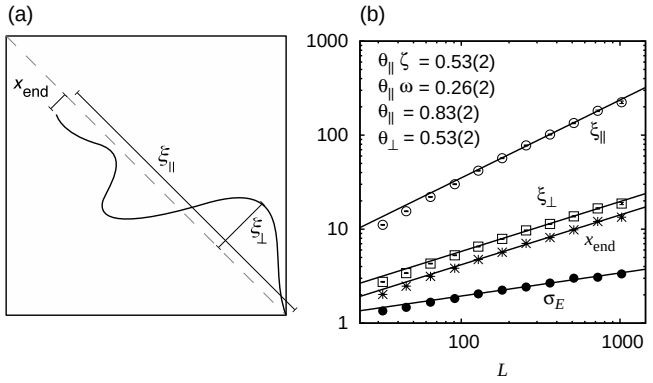

FIG. 3: (a) Sketch of $\xi_\parallel$, $\xi_\perp$ and $x_{\rm end}$. (b) Plot shows $\xi_\parallel$ (red. $\chi^2 = 1.1$), $\xi_\perp$ (red. $\chi^2 = 1.5$), $x_{\rm end}$ (red. $\chi^2 = 2.1$) and σ_E (red. $\chi^2 = 3.8$) as a function of L. Merely system sizes from $L = 181$ to 724 have been considered for the power-law regression curves. The measurements are taken at the estimated value of the critical point $\rho_c = 0.3789$.

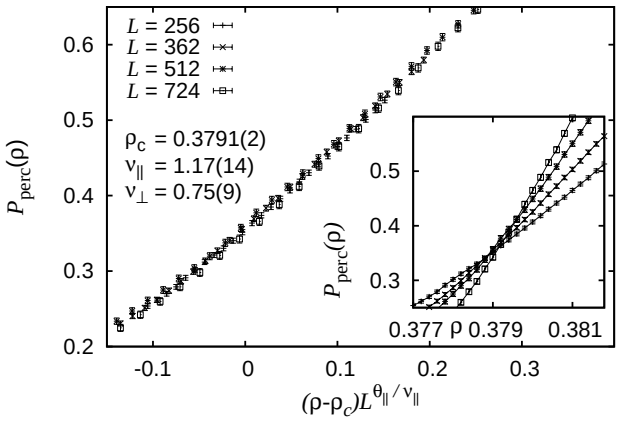

FIG. 4: Percolation probability $P_{\rm perc}(\rho)$ as a function of ρ in the vicinity of the critical point (inset). The data is collapsed to one curve by using the scaling assumption Eq. 5 (main plot).

we could study rather large system sizes in the range $L = 256$ to $L = 724$ with good statistics: The data have been obtained by averaging over 20000 ($L = 256$), 16000 ($L = 362$), 10000 ($L = 512$) and 8000 ($L = 724$) realizations of the disorder, respectively.

Fig. 4 shows the percolation probability $P_{\rm perc}(\rho)$ as a function of the disorder parameter ρ as well as the rescaled data collapse. Since the percolation probability is a dimensionless quantity, $b = 0$ is set in Eq. 5. The estimates $\rho_c = 0.3791(2)$, $\nu_\parallel = 1.17(14)$ and $\nu_\perp = 0.75(9)$ provide the best data collapse with quality $S = 1.2$, which denotes the mean-square distance of the data points to the unknown scaling function in units of the standard error [22].

We have also measured the average number of lattice-spanning objects $\langle N\rangle$, see Fig. 5. Note that, in contrast

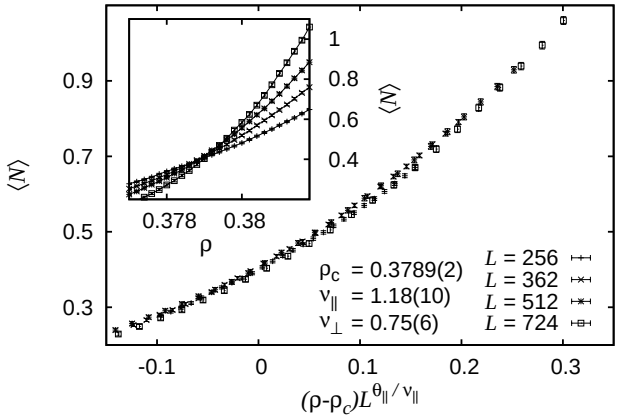

FIG. 5: Average number of spanning loops $\langle N\rangle$ as a function of ρ in the vicinity of the critical point (inset). The data is collapsed to one curve by using the scaling assumption Eq. 5 (main plot).

to standard percolation, more than one object can be spanning. By using again the data-collapse approach, we have found $\rho_c = 0.3789(2)$, $\nu_\parallel = 1.18(10)$ and $\nu_\perp = 0.75(6)$ with quality $S = 2.3$.

Another quantity that has been under scrutiny is the order parameter

$$P_{\rm node} \equiv \frac{\langle l\rangle}{L^d}, \tag{6}$$

which is the probability that an edge belongs to either a percolating loop or percolating path. The total number of all edges that belong to the percolating objects is given by l. $d = 2$ signifies the dimension of the lattice. The asymptotic behavior of the order parameter is governed by an additional critical exponent β, the percolation strength [23]. As evident from Fig. 6, we have found $\rho_c = 0.3788(2)$, $\nu_\parallel = 1.18(18)$, $\nu_\perp = 0.75(11)$ and $\beta = 1.42(21)$ with quality $S = 1.3$. It should be noted that several combinations of ρ_c and the exponents provide valid data collapses. Therefore, we considered $P_{\rm node}$ versus L at the critical point (plot not shown here), which exhibits only one fitting parameter. We found for large system sizes a power law behavior, which is compatible with $\beta = 1.42(21)$, which we therefore take as final estimate.

Next, we consider the associated finite-size susceptibility

$$\chi_L = L^{-d}(\langle l^2\rangle - \langle l\rangle^2), \tag{7}$$

whose asymptotic behavior is guided by the critical exponent γ. As can be seen from Fig. 7, the best data collapse is provided by $\rho_c = 0.3789(3)$, $\nu_\parallel = 1.18(26)$, $\nu_\perp = 0.76(17)$ and $\gamma = 0.00(5)$ with quality $S = 0.8$.

Right at the critical point, we studied the distribution of path-lengths excluding the lattice-spanning ones. As

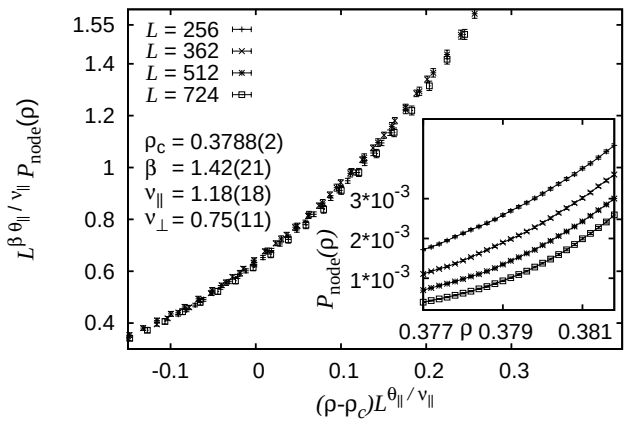

FIG. 6: Order parameter $P_{\rm node}(\rho)$ as a function of ρ in the vicinity of the critical point (inset). The data is collapsed to one curve by using the scaling assumption Eq. 5 (main plot).

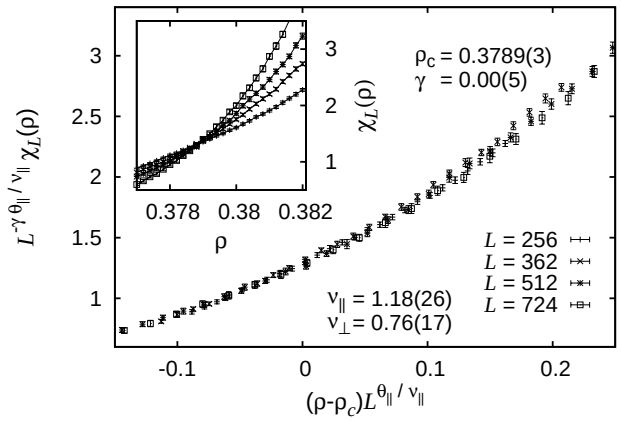

FIG. 7: Fluctuations of the order parameter $\chi_L(\rho)$ over ρ in the vicinity of the critical point (inset). The data is collapsed to one curve by using the scaling assumption Eq. 5 (main plot).

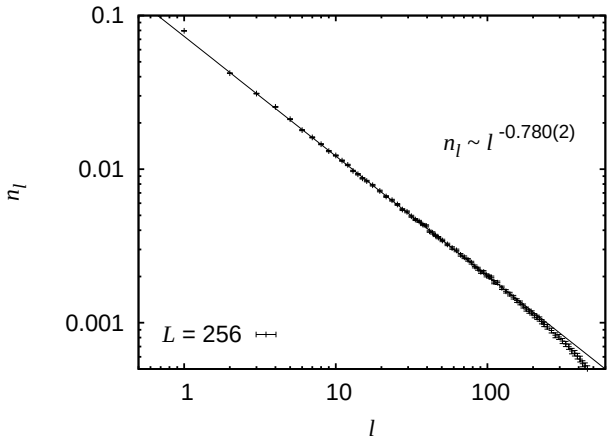

FIG. 8: Distribution of the path lengths l at the critical point excluding those which percolate. 1200000 realizations of the disorder have been considered. For the fit (red. $\chi^2 = 1.0$) path lengths from $l = 2$ to 100 have been taken into account only.

evident from Fig. 8, the distribution is in good agreement with a power law decay $n_l \sim l^{-\tau}$ with $\tau = 0.780(2)$.

NWP is defined as a global optimization problem (cf. Sec. II) to find the minimally weighted configuration consisting of loops plus one path. Since in the directed polymer problem [14] minimally weighted paths are also selected by global optimization in a random media, these two models might be related. The DPRM can be described as follows: A weighted square lattice, in which all edges carry a positive weight, gets cut along its diagonal and then it is oriented as a triangle, whose right angle is up. Then all edges become directed and point either to bottom right or bottom left. On such a lattice, for a given realization of the disorder, one looks for the minimally weighted path that goes from the apex to the base. It has been shown in Ref. [24] that $\zeta^\circ = 2/3$, where ζ° is the roughness exponent defined by $D \sim t^{\zeta^\circ}$. D describes the mean distance between the base center and the endpoint of the path and t is the size of the triangle. Furthermore, it is also shown in Ref. [24] that $\omega^\circ = 1/3$, which is defined by $\sigma_E \sim t^{\omega^\circ}$. σ_E denotes the standard deviation of the weight of the optimal path. A relation between these two exponents is given by the scaling relation $\omega^\circ = 2\zeta^\circ - 1$ [24]. There are some differences between the optimal path in DPRM and the path that appears in directed NWP. First of all, the directed NWP includes the disorder parameter ρ which allows us to investigate a percolation transition, which is completely absent for DPRM, since all paths are system spanning by construction. There are also smaller technical differences: For the directed NWP, one looks for an optimal configuration of loops plus one path in NWP. The loops, which cannot be crossed by the path, have to be negatively weighted as well and, therefore, block several negatively weighted edges that cannot be picked up by the path. Thus, this path can not be considered as optimal on its own. Furthermore, while the lengths of the paths in DPRM are always equal, the lengths of the paths in NWP differ considerably.

Nevertheless, in spite of one big and the two smaller differences, directed NWP and DPRM exhibit some scaling which is comparable. This is not unnatural, since both models describe some optimal paths in disordered lattices: In order to compare both models, we identify $D \leftrightarrow x_{\rm end}$, where $x_{\rm end}$ is the distance between the endpoint of the path and the line of predominant direction (cf. Fig. 3(a)) and $t \leftrightarrow \xi_\parallel$. Then we consider $x_{\rm end} \sim \xi_\parallel^\zeta \sim L^{\theta_\parallel \zeta}$ and $\sigma_E \sim \xi_\parallel^\omega \sim L^{\theta_\parallel \omega}$ for the NWP model. As evident from Fig. 3(b), $x_{\rm end}$ scales with $\theta_\parallel \zeta = 0.53(2)$ and σ_E with $\theta_\parallel \omega = 0.26(2)$. Consequently, $\omega = 0.31(3)$ and $\zeta = 0.64(4)$, which are in good agree-

ment with the exponents of the DPRM model.

Note that in our model the path is included to determine its geometrical properties, in particular its extension parallel and perpendicular to the preferred (diagonal) lattice direction. Nevertheless, we have also performed simulations for the model *without* a path, just to study the percolation properties of loops alone. All results (for somehow smaller system sizes, not shown here) for the percolation properties remain the same within error bars.

IV. SUMMARY

In this work with have studied the directed variant of the negative-weight percolation model. This model defined as a global optimization problem. The model can be studied numerically efficiently, since a mapping to the minimum-weight perfect matching problem exist, such that fast polynomial-time optimization algorithms can be applied. Thus, large systems can be studied numerically with good statistics giving rise to high-quality results. The model exhibits a continuous phase transition, that is characterized by the appearance of loops and a path where at least one of them is large, i.e., system-spanning. We have studied this percolation transition by extended numerical simulations and their analysis based on a finite-size scaling method. By investigating several cluster-related observables we found estimates for the percolation threshold, which we summarized here as $\rho_c = 0.3789(3)$, several critical exponents $\nu_\parallel = 1.18(10)$, $\nu_\perp = 0.75(6)$, $\beta = 1.42(21)$, $\gamma = 0.00(5)$ and an exponent that describes the power-law decay of the path-length distribution $\tau = 0.780(2)$. For the values of the correlation lengths, we have taken the estimates which yielded the smallest statistical error bars (from the data collapse of the average number $\langle N \rangle$ of percolating loops). These values are compatible with the estimates from the scaling of other quantities. Finally, we tested the scaling relation $2\beta = \nu_\parallel + \nu_\perp - \gamma$ [25], which is a standard relation for directed percolation. For the left side we get 2.84(42) while for the right side we get 1.93(21). Thus within one-sigma, the scaling relation is not fulfilled, while within two-sigma, the left and right side are compatible. Thus, it is presently not fully clear whether the scaling relation is fulfilled. If not, it could be due to the fact that the percolating objects are line-like rather than bulk-like. Note that for standard directed percolation near a wall, for the results obtained using a series expansion the scaling relation is clearly violated [26]. Nevertheless, in the case of a violation it would be different from the undirected NWP case, where the standard scaling relations for percolation hold [6, 8].

Additionally, we have shown that the directed negative-weight percolation model is related to directed polymers in random media (DPRM), although the DPRM does not exhibit a percolation transition (except when diluting the system where just the standard percolation transition appears.)

Acknowledgments

Financial support was obtained via the Lower Saxony research network "Smart Nord" which acknowledges the support of the Lower Saxony Ministry of Science and Culture through the "Niedersächsisches Vorab" grant program (grant ZN 2764/ ZN 2896). The simulations were performed at the *HERO* cluster for scientific computing of the University of Oldenburg jointly funded by the DFG (INST 184/108-1 FUGG) and the ministry of Science and Culture (MWK) of the Lower Saxony State.

[1] H. E. Stanley, Rev. Mod. Phys. **71**, 358 (1999).
[2] D. Stauffer, Physics Reports **54**, 1 (1979).
[3] D. Stauffer and A. Aharony, *Introduction to Percolation Theory* (Taylor & Francis, 1992).
[4] C. M. Fortuin and P. W. Kasteleyn, Physica **57**, 536 (1972).
[5] H. Hinrichsen, Adv. Phys. **49**, 815 (2000).
[6] O. Melchert and A. K. Hartmann, New. J. Phys. **10**, 043039 (2008).
[7] L. Apolo, O. Melchert, and A. K. Hartmann, Phys. Rev. E **79**, 031103 (2009).
[8] O. Melchert, L. Apolo, and A. K. Hartmann, Phys. Rev. E **81**, 051108 (2010).
[9] O. Melchert and A. K. Hartmann, Eur. Phys. J. B **80**, 155 (2011).
[10] O. Melchert, A. K. Hartmann, and M. Mézard, Phys. Rev. E **84**, 041106 (2011).
[11] G. Claussen, O. Melchert, and A. K. Hartmann, Phys. Rev. E **86**, 056708 (2012).
[12] C. Norrenbrock, O. Melchert, and A. K. Hartmann, Phys. Rev. E **87**, 032142 (2013).
[13] O. Melchert, C. Norrenbrock, and A. K. Hartmann, Physics Procedia **57**, 58 (2014).
[14] M. Kardar and Y.-C. Zhang, Phys. Rev. Lett. **58**, 2087 (1987).
[15] O. Melchert, *PhD thesis* (not published, 2009).
[16] W. Cook and A. Rohe, INFORMS J. Computing **11**, 138 (1999).
[17] A. K. Hartmann and H. Rieger, *Optimization Algorithms in Physics* (Wiley-VCH, Weinheim, 2001).
[18] O. Melchert and A. K. Hartmann, Phys. Rev. B **76**, 174411 (2007).
[19] For the calculation of minimum-weighted perfect matchings we use Cook and Rohes blossom4 extension to the Concorde library., URL `http://www2.isye.gatech.edu/~wcook/blossom4/`.
[20] S. Sinha and S. B. Santra, Preprint: arXiv:0807.2300v1 (2008).
[21] K. Binder and D. W. Herrmann, *Monte Carlo Simulation in Statistical Physics: An Introduction* (Springer, Berlin,

2002).
[22] O. Melchert, Preprint: arXiv:0910.5403v1 (2009).
[23] D. Stauffer and A. Aharony, *Introduction to Percolation Theory* (Taylor and Francis, London, 1994).
[24] D. A. Huse and C. Henley, Phys. Rev. Lett. **54**, 2708 (1985).
[25] J. W. Essam, A. J. Guttmann, and D. K., J. Phys. A **21**, 3815 (1988).
[26] I. J. J. W. Essam, A. J. Guttmann and D. TanlaKishani, J. Physics A **29**, 1619 (1996).